

## **Electronic Supplementary Information (ESI)**

### **Switching from positive to negative thermal expansion in a tetrayne-diol compound**

Tapaswini Sethi<sup>a</sup> and Dinabandhu Das<sup>\*a</sup>

School of Physical Sciences, Jawaharlal Nehru University, New Delhi-110067, India

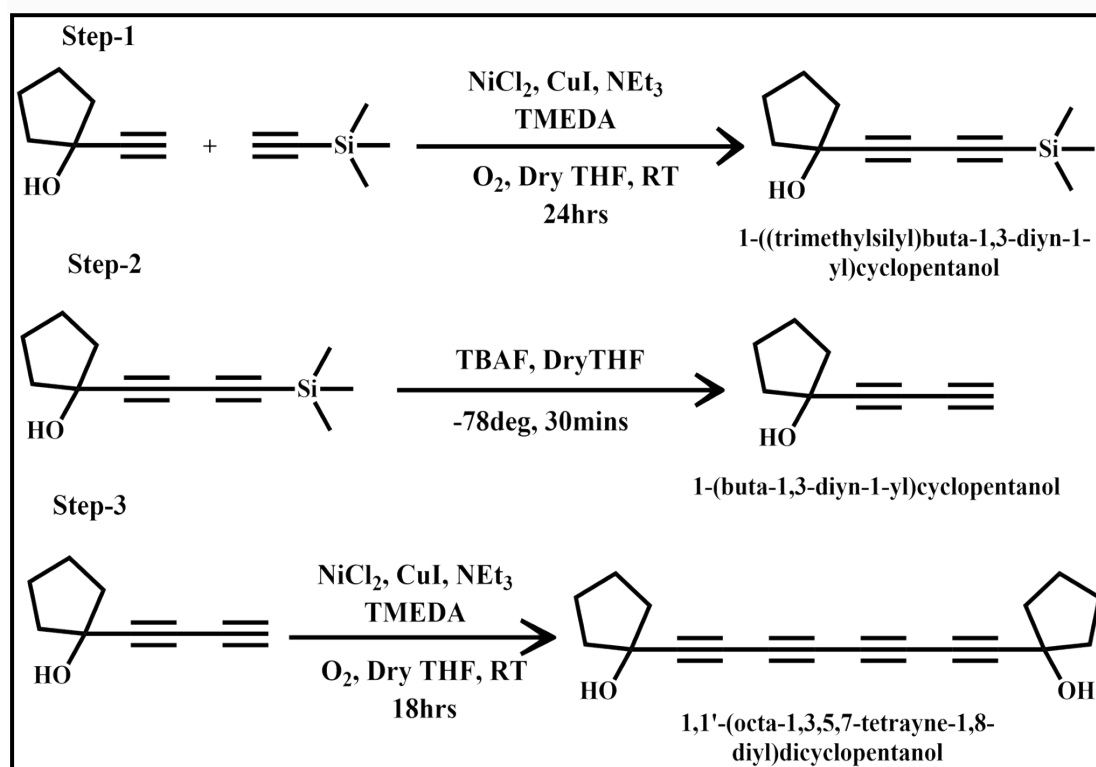
[jnu.dinu@gmail.com](mailto:jnu.dinu@gmail.com)

## TABLE OF CONTENT

1. Experimental Section
2.  $^1\text{H}$ -NMR Spectra
3.  $^{13}\text{C}$ -NMR Spectra
4. FT-IR and UV-Vis Spectra
5. Powder X-Ray Diffraction Study
6. Thermogravimetric Analysis (TGA)
7. Differential Scanning calorimetry (DSC)
8. Single crystal X-Ray Diffraction Study
9. Variable Temperature X-Ray Diffraction Study
10. Thermal ellipsoid plots of Asymmetric Units at different temperature
11. Change in Unit cell parameters of the crystal structures of (1) with temperature
12. Change in Hydrogen bonding parameters with change in temperature
13. Change in C-H $\cdots\pi$  interaction with change in temperature
14. Change in interlayer distance with change in temperature
15. Change in  $\vartheta$ ,  $\varphi$ , X and Y with change in temperature
16. Calculation of Thermal Expansion Coefficients by PASCAL Program
17. Measurement of torsion angle and Cremer & Pople ring Puckering Parameters with change in temperature from 100-350K
18. Variation of anisotropic displacement parameters (U11, U22, U33) of carbon atoms with temperature
19. References

## 1. Experimental Section

All the chemicals and solvents were purchased from local chemical sources and used as received. THF was dried using Sodium and benzophenone. Solvent used for column chromatography has been used after distillation. Compound **1** was synthesized according to the reported literature procedure<sup>1</sup>.



**Scheme S1:** General method for the synthesis of Compound **1**

**Step-1:** CuI (5 mol%) and anhydrous NiCl<sub>2</sub> (5 mol%) were dissolved in dry THF (4 mL) and TMEDA (20 mol%), NEt<sub>3</sub> (5 mol%) was added to it and the solution was stirred for 2 min at room temperature. 1-Ethynylcyclopentanol (570μL, 550.8mg, 5mmol) and (Trimethylsilyl)acetylene (130μL, 98.22mg, 1mmol) were added subsequently and the reaction mixture was stirred under air for 24 hours at room temperature. After completion of the reaction, as indicated by TLC, the mixture was concentrated in vacuo and the compound was extracted by using ethyl acetate and water. After collecting the ethyl acetate layer the solvent was evaporated and the

crude compound was purified by column chromatography using ethyl acetate and hexane as mobile phase. After purification the compound has been got with 70% yield with respect to the (Trimethylsilyl)acetylene.

**Step-2:** The resultant compound from step-1 *i.e.* 1-((trimethylsilyl)buta-1,3-diyn-1-yl)cyclopentanol (105mg, 0.5mmol) was stirred in dry THF at at  $-78\text{ }^{\circ}\text{C}$  under  $\text{N}_2$  atmosphere. Then to it TBAF (5.5mL, 1M solution in THF, 5.5mmol) was added slowly. After 30 min, the reaction mixture was quenched with saturated  $\text{NH}_4\text{Cl}$  and extracted with ethyl acetate. The combined organic extracts were washed with water and brine sequentially and dried over anhydrous  $\text{MgSO}_4$  and concentrated under reduced pressure. The product is used for the next step without further purification.

**Step-3:**  $\text{CuI}$  (5 mol%) and anhydrous  $\text{NiCl}_2$  (5 mol%) were dissolved in dry THF (4 mL) and TMEDA (20 mol%),  $\text{NEt}_3$  (5 mol%) was added to it and the solution was stirred for 2 min at room temperature. To it THF solution of the product got from step 2 *i.e.* 1-(buta-1,3-diyn-1-yl)cyclopentanol (50 $\mu\text{L}$ , 55mg, 0.4mmol) was added slowly and stirred under air for 24 hours at room temperature. After completion of the reaction, as indicated by TLC, the mixture was concentrated in vacuum and the compound was extracted by using ethyl acetate and water. After collecting the ethyl acetate layer the solvent was evaporated and the crude compound was purified by column chromatography using ethyl acetate and hexane as mobile phase. After purification the compound has been got with 85% yield with respect to the 1-(buta-1,3-diyn-1-yl)cyclopentanol. Exact melting point of the compound could not be measured due to decomposition. Melting point measured in capillary is about  $120\text{ }^{\circ}\text{C}$  to  $122\text{ }^{\circ}\text{C}$  along with decomposition.

The compound was then characterized by using  $^1\text{H-NMR}$ ,  $^{13}\text{C-NMR}$ , FT-IR, SCXRD. The phase purity of the sample was checked through PXRD. For thermal stability

Thermogravimetric analysis (TGA) and Differential scanning calorimetry (DSC) have been performed. The compound was crystallized in different solvents and also with mixture of solvents. The crystals of compound **1** were formed in the 1:1 mixture of ethyl acetate and chloroform. After complete evaporation of solvent plate shaped pale yellow color crystals were formed.

## 2. $^1\text{H-NMR}$ Spectra

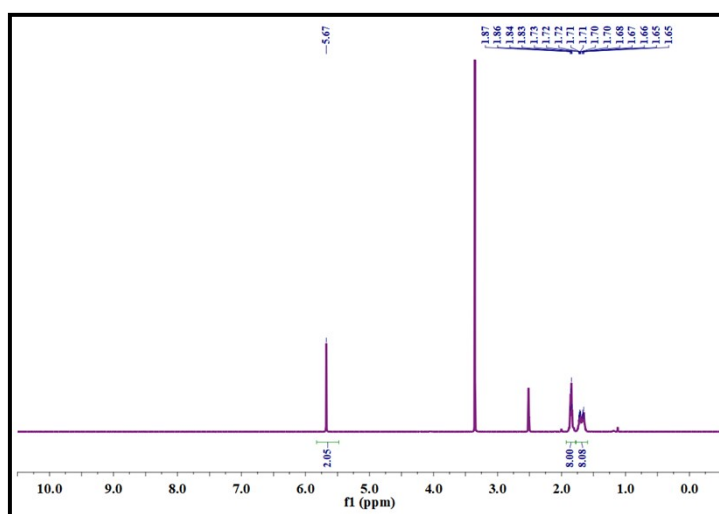


**Figure S1**  $^1\text{H-NMR}$  Spectra of **1** (500MHz,  $\text{DMSO-d}_6$ ):  $\delta$  1.65 (m, 8H),  $\delta$  1.83 (m, 8), 5.67 (s, 2H)

## 3. $^{13}\text{C-NMR}$ Spectra

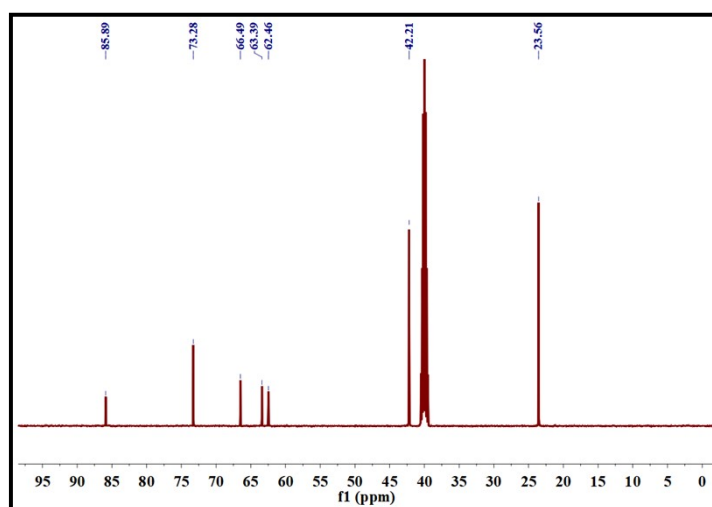


**Figure S2**  $^{13}\text{C-NMR}$  Spectra of **1** (500MHz,  $\text{DMSO-d}_6$ ):  $\delta$  23.56, 42.21, 62.46, 63.39, 66.49, 73.28, 85.89.

#### 4. FT-IR and UV-Vis Spectra

FT-IR spectra the synthesized compound was collected from 400 to 4000  $\text{cm}^{-1}$  on a Shimadzu IRAffinity-1SWL instrument. The instrument is connected with LabSolutions IR control software.

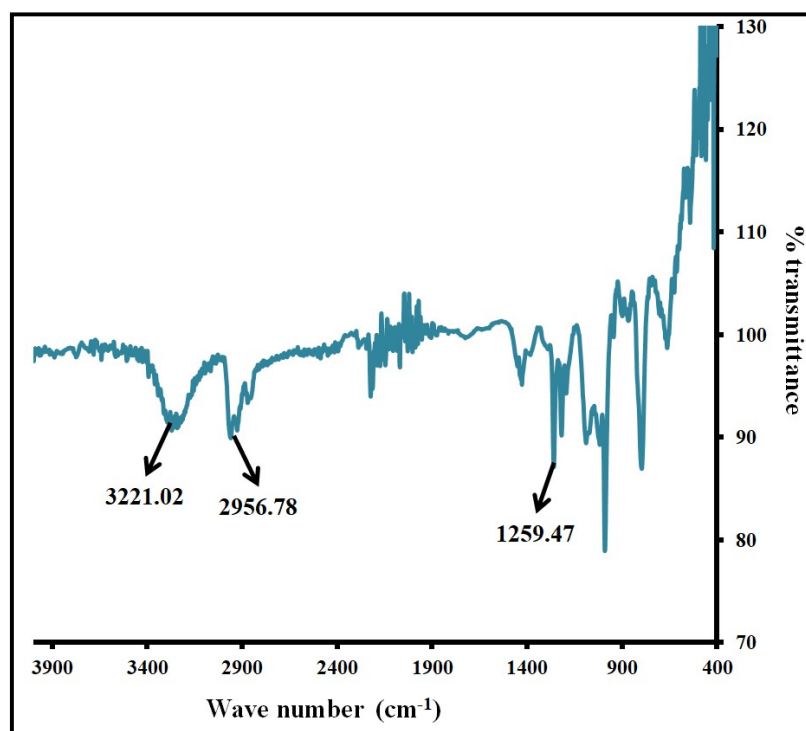


**Figure S3.** FT-IR Spectra of 1 recorded in Shimadzu (IR Affinity-1SWL).

#### UV-Visible Spectra of Compound 1

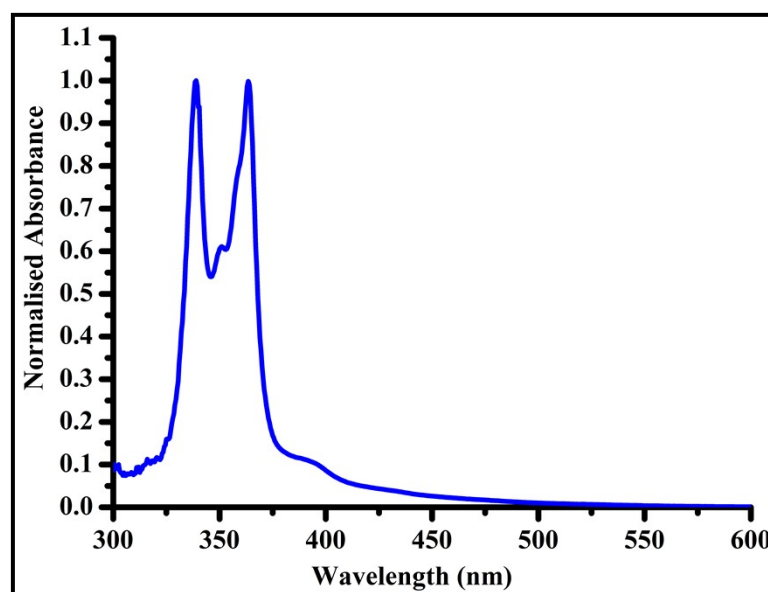


**Figure S4.** UV-Visible Spectra of 1 by taking 6.26mM solution in THF solvent

## 5. Powder X-Ray Diffraction Study

The phase purity of **1** was analyzed by comparing the experimental PXRD pattern with the simulated PXRD pattern obtained from the crystal structure data. The measurement of powder X-ray diffraction study was carried out on Rigaku powder X-ray diffractometer (Miniflex600) using CuK $\alpha$  radiation ( $\lambda = 1.54059 \text{ \AA}$ ). For taking experimental PXRD pattern the powder sample was loaded on a sample holder and the measurement was carried out at room temperature from  $5^\circ$  to  $40^\circ$  ( $2\theta$  value) at a scan rate of  $2^\circ/\text{min}$ .

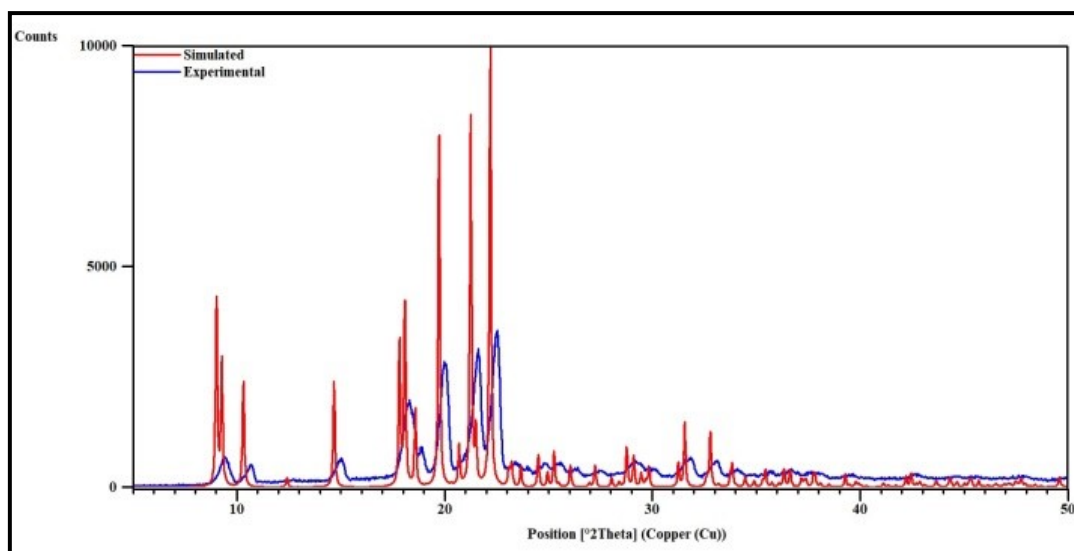


**Figure S5** Comparison of experimental PXRD pattern of **1**(blue) with the simulated one (red)

## 6. Thermogravimetric Analysis

The TGA measurement of **1** was performed by taking 2.5mg sample in a alumina pan and experiment has been performed on Mettler Toledo equipped with Minichiller MT/230 under nitrogen atmosphere (flow rate:20 ml /minute and at a scan rate of  $5^\circ\text{C} / \text{min}$ .), using a software STARe version 13.00. The TGA analysis reveals that the sample experiences a mass loss that begins at  $90^\circ\text{C}$ .

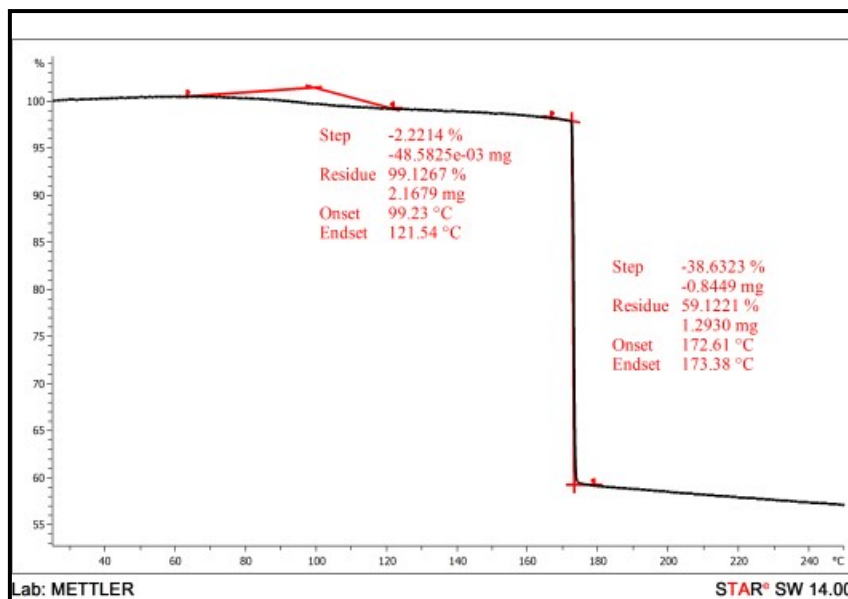


**Figure S6.** TGA thermogram of **1**

## 7. Differential scanning calorimetry (DSC)

The differential scanning calorimetric (DSC) measurement of **1** has been carried out in a sealed aluminium pan in the Mettler-Toledo DSC instrument. The instrument was equipped with HUBER TC100-MT chiller and STARe software version 13.00. The measurement was carried out from 25°C to 180°C at the heating rate of 5°C/min under a N<sub>2</sub> gas segment with a flow rate of 20ml/min. The DSC thermogram reveals that no other phase is present in case of **1** till 90°C.

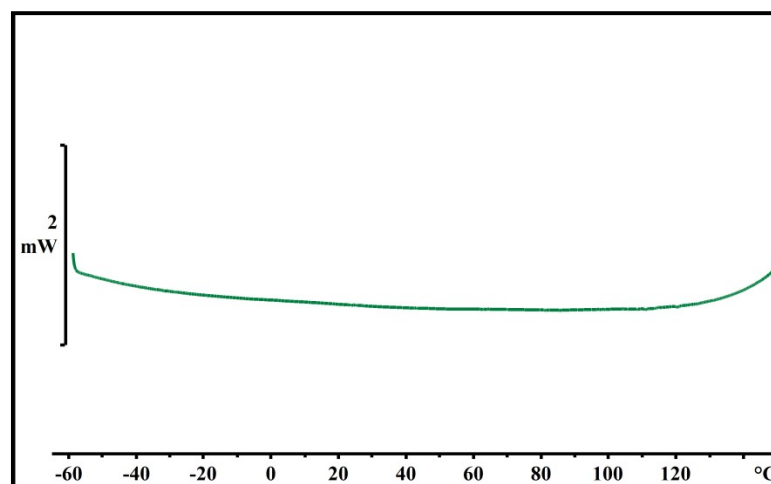


**Figure S7.** DSC thermogram of **1**



## 8. Single crystal X-Ray Diffraction Study

For routine data collection a suitable single crystal of **1** was mounted on goniometer head using nylon loop and single crystal X-Ray diffraction data has been taken on Bruker D8 Quest single crystal X-ray diffractometer equipped with a microfocus anode ( $\text{MoK}\alpha$ ) and a PHOTON 100 CMOS detector. The data was integrated and scaled using the Bruker suite programs.<sup>2</sup> Structure was solved by direct method and refined using SHELXL.<sup>3,4</sup>

## 9. Variable Temperature X-Ray Diffraction Study

For variable temperature single crystal X-Ray diffraction study a suitable single crystal was glued with epoxy glue on top of a glass fiber. The single-crystal data was collected from 150K to 350K at intervals of 50K each. All the data at each temperature was integrated and scaled using the Bruker suite programs.<sup>2</sup> Structure was solved by direct method and refined using SHELXL<sup>3,4</sup> and X-Seed software.<sup>5</sup> Crystallographic data and final refinement details are given in Table S1.

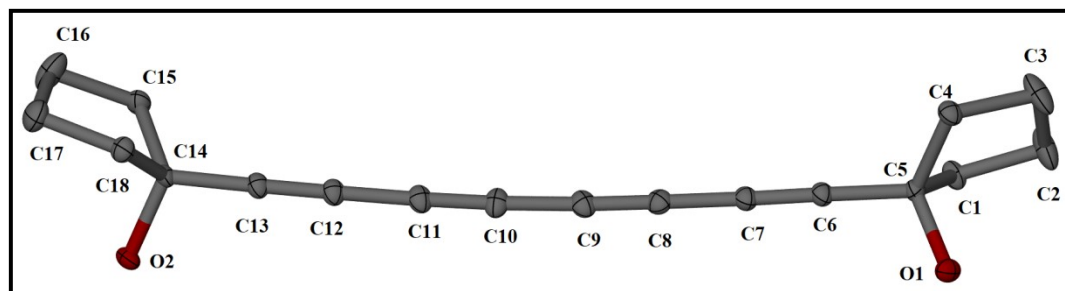
**Table S1:** Crystallographic data of **1** from 100K to 350K.

Compound	100K	150K	200K	250K	300K	350K
Moiety formula	$\text{C}_{18}\text{H}_{18}\text{O}_2$	$\text{C}_{18}\text{H}_{18}\text{O}_2$	$\text{C}_{18}\text{H}_{18}\text{O}_2$	$\text{C}_{18}\text{H}_{18}\text{O}_2$	$\text{C}_{18}\text{H}_{18}\text{O}_2$	$\text{C}_{18}\text{H}_{18}\text{O}_2$
Crystal system	Orthorhombic	Orthorhombic	Orthorhombic	Orthorhombic	Orthorhombic	Orthorhombic
Space group	<i>Aba2</i>	<i>Aba2</i>	<i>Aba2</i>	<i>Aba2</i>	<i>Aba2</i>	<i>Aba2</i>
<i>a</i> /Å	19.6427(17)	19.6437(13)	19.6451(12)	19.6363(11)	19.6266(10)	19.6202(13)
<i>b</i> /Å	18.5826(16)	18.7051(12)	18.8313(11)	18.9629(10)	19.0995(9)	19.2474(12)
<i>c</i> /Å	8.2741(6)	8.2918(5)	8.3108(4)	8.3326(4)	8.3570(4)	8.3912(5)
<i>a</i> /(°)	90	90	90	90	90	90
<i>β</i> /(°)	90	90	90	90	90	90
<i>γ</i> /(°)	90	90	90	90	90	90
<i>V</i> /Å <sup>3</sup>	3020.1(4)	3046.7(3)	3074.5(3)	3102.4(3)	3132.7(3)	3168.8(3)
<i>Z</i>	8	8	8	8	8	8

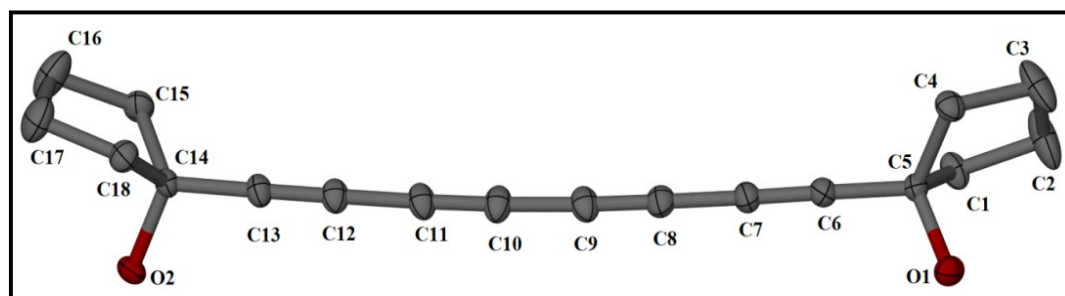
$D_{\text{cal}}/\text{g cm}^{-3}$	1.171	1.161	1.151	1.140	1.129	1.116
T/K	100(2)	150(2)	200(2)	250(2)	300(2)	350(2)
$\mu/\text{mm}^{-1}$	0.075	0.074	0.074	0.073	0.072	0.072
$F_{000}$	1136	1136	1136	1136	1136	1136
Reflections measured	31321	31502	32348	33380	33578	34233
Unique reflections	3552	3580	3618	3695	3718	3785
Observed reflections	3406	3368	3287	3139	3121	2821
Parameters	189	189	189	189	189	189
$R_{\text{int}}$	0.0444	0.0434	0.0444	0.0455	0.0434	0.0460
final $R$ ( $I > 2\sigma(I)$ )	0.0365	0.0414	0.0448	0.0469	0.0510	0.0572
final $R$ (all data)	0.0388	0.0450	0.0515	0.0593	0.0638	0.0799
GOF on $F^2$	1.051	1.082	1.044	1.047	1.089	1.063
CCDC No.	2366943	2366944	2366945	2366946	2366947	2366948

Note. All parameters are calculated using PLATON.<sup>6a</sup>

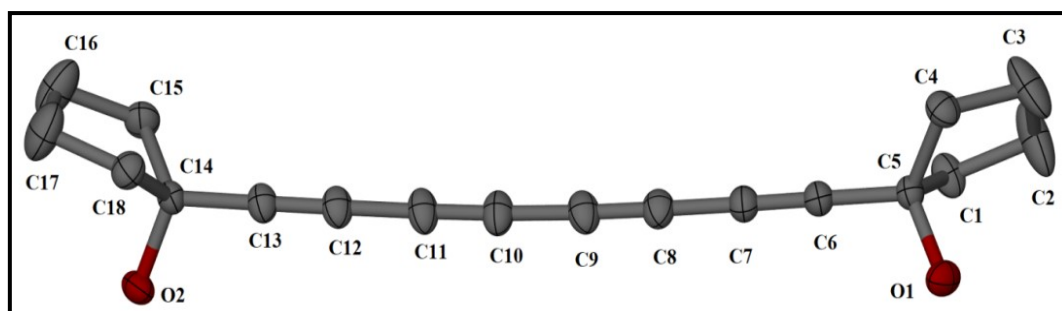
### 10. Thermal ellipsoid plots of Asymmetric Units at different temperature



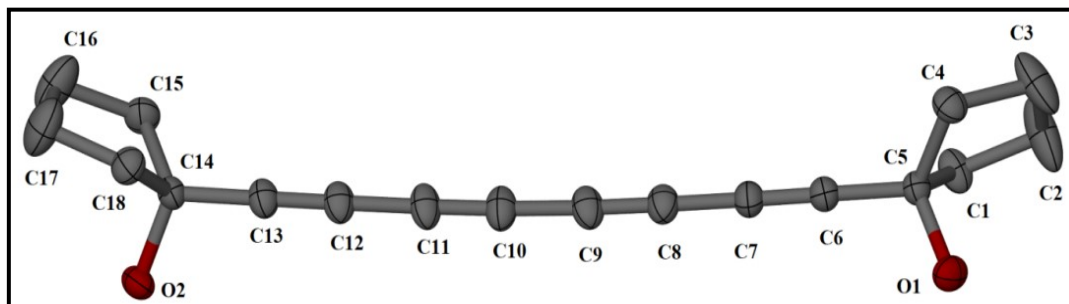
100K



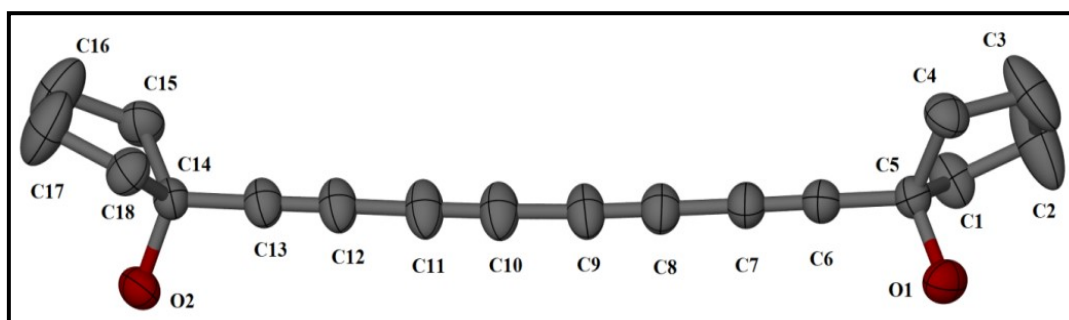
150K



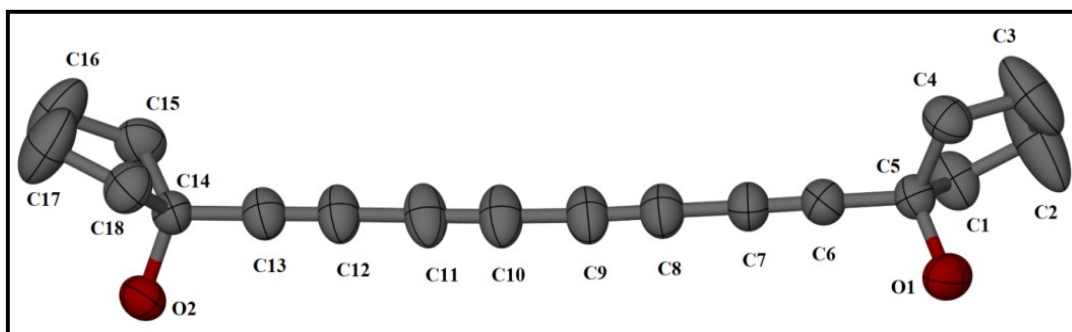
200K



250K



300K



350K

**Figure S8** Thermal ellipsoid plot of the asymmetric unit of crystal structure of the compound **1** at different temperature with 40% probability.

## 11. Change in Unit cell parameters of the crystal structures of (1) with temperature

Table S2 Change in unit cell parameters with change in temperature

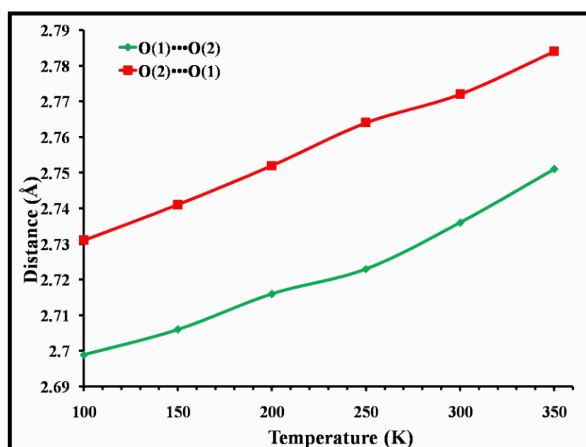
Temperature (K)	$a$ (Å)	$b$ (Å)	$c$ (Å)	$\alpha=\beta=\gamma$ (°)	Volume(V)(Å <sup>3</sup> )
100	19.6427(17)	18.5826(16)	8.2741(6)	90	3020.15
150	19.6437(13)	18.7051(12)	8.2918(5)	90	3046.72
200	19.6451(12)	18.8313(11)	8.3108(4)	90	3074.52
250	19.6363(11)	18.9629(10)	8.3326(4)	90	3102.74
300	19.6266(10)	19.0995(9)	8.3570(4)	90	3132.69
350	19.6202(13)	19.2474(12)	8.3912(5)	90	3168.83

## 12. Change in Hydrogen bonding parameters with change in temperature

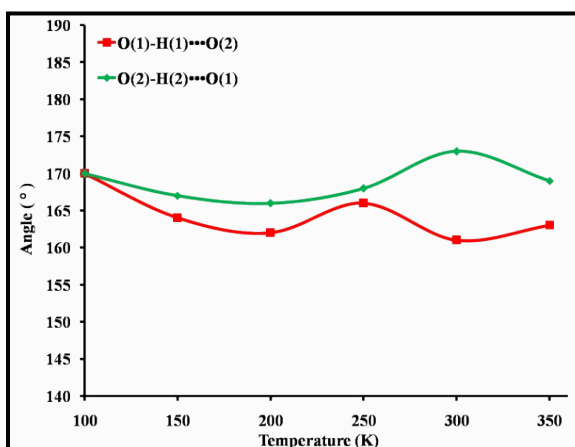
Table S3 Change in hydrogen bonding parameters with change in temperature

Donor – H ...Acceptor		100K	150K	200K	250K	300K	350K
<b>O(1)-H(1)...O(2)</b>	O(1)-H(1)	0.84(3)	0.89(4)	0.99(4)	0.98(4)	0.96(6)	0.97(8)
	H(1)...O(2)	1.87(3)	1.84(4)	1.76(4)	1.77(4)	1.81(6)	1.81(8)
	O(1) - O(2)	2.6989(19)	2.706(2)	2.716(2)	2.723(3)	2.736(3)	2.751(3)
	$\angle$ O(1)- H(1)...O(2)	170(3)	164(3)	162(3)	166(3)	161(5)	163(7)

<b>O(2)-H(2)···O(1)</b>	O(2)-H(2)	0.78(3)	0.84(3)	0.86(4)	0.88(3)	0.86(4)	0.89(5)
	H(2)···O(1)	1.96(3)	1.92(3)	1.92(4)	1.90(3)	1.92(4)	1.91(5)
	O(2) - O(1)	2.731(2)	2.741(2)	2.752(2)	2.764(3)	2.772(3)	2.784(4)
	$\angle$ O(2)- H(2)···O(1)	170(3)	167(3)	166(3)	168(3)	173(3)	169(4)



(a)



(b)

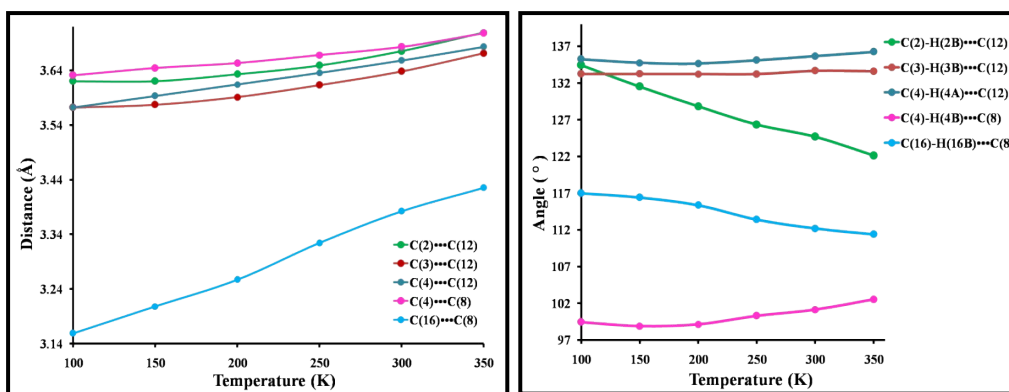
**Figure S9** Change in hydrogen bonding parameters (a) O-H···O bond length; (b) O-H···O bond angle with change in temperature

### 13. Change in C-H··· $\pi$ interaction with change in temperature

**Table S4** Change in C – H··· $\pi$  interactions with change in temperature

C – H ... $\pi$		100K	150K	200K	250K	300K	350K
<b>C(2)- H(2B)···C(12)</b>	C(2)-H(2B) (Å)	0.990	0.990	0.990	0.980	0.971	0.970
	H(2B)···C(12) (Å)	2.858	2.887	2.930	2.982	3.035	3.101
	C(2)-C(12) (Å)	3.620(3)	3.620(3)	3.633(5)	3.649(6)	3.675(7)	3.709(8)
	$\angle$ C(2)- H(2B)···C(12) (°)	134.42	131.52	128.81	126.32	124.67	122.12

<b>C(3)- H(3B)···C(12)</b>	C(3)-H(3B) (Å)	0.990	0.990	0.990	0.979	0.970	0.970
	H(3B)···C(12) (Å)	2.821	2.825	2.840	2.871	2.901	2.934
	C(3)-C(12) (Å)	3.572(3)	3.577(4)	3.591(5)	3.613(5)	3.638(6)	3.671(8)
	$\angle$ C(3)- H(3B)···C(12) (°)	133.24	133.23	133.21	133.20	133.65	133.58
<b>C(4)- H(4A)···C(12)</b>	C(4)-H(4A) (Å)	0.990	0.990	0.990	0.980	0.970	0.970
	H(4A)···C(12) (Å)	2.800	2.826	2.849	2.874	2.901	2.921
	C(4)-C(12) (Å)	3.572(2)	3.593(3)	3.614(4)	3.635(4)	3.658(5)	3.683(6)
	$\angle$ C(4)- H(4A)···C(12) (°)	135.23	134.74	134.63	135.10	135.64	136.23
<b>C(4)- H(4B)···C(8)</b>	C(4)-H(4B) (Å)	0.990	0.990	0.990	0.980	0.970	0.970
	H(4B)···C(8) (Å)	3.334	3.356	3.363	3.364	3.370	3.374
	C(4)-C(8) (Å)	3.631	3.644(3)	3.653(4)	3.668(4)	3.683	3.708(6)
	$\angle$ C(4)- H(4B)···C(8) (°)	99.45	98.9	99.14	100.31	101.15	102.52
<b>C(16)- H(16B)···C(8)</b>	C(16)-H(16B) (Å)	0.990	0.990	0.991	0.980	0.969	0.970
	H(16B)···C(8) (Å)	3.159	3.208	3.257	3.324	3.382	3.425
	C(16)-C(8) (Å)	3.715(3)	3.755(4)	3.788(5)	3.820(5)	3.854(6)	3.886(7)
	$\angle$ C(16)- H(16B)···C(8) (°)	116.97	116.42	115.36	113.40	112.18	111.4



(a)

(b)

**Figure S10** Change in C – H •••π interactions (a) C – H •••π bond length; (b) C – H •••π bond angle with change in temperature

#### 14. Change in interlayer distance with change in temperature

**Table S5** Change interlayer distance with change in temperature

Temp.(K)	Distance between two layers (C14-C14)(Å)
100	10.171(2)
150	10.230(3)
200	10.292(3)
250	10.356(3)
300	10.424(4)
350	10.499(4)

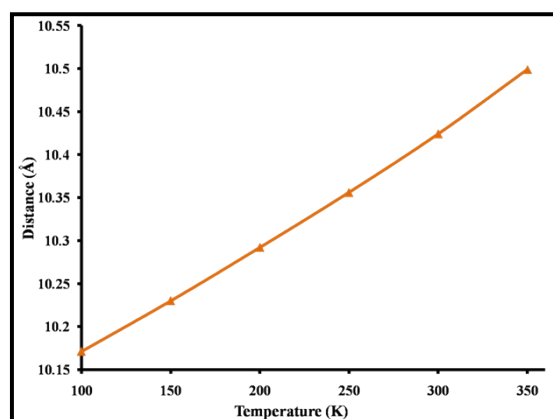


**Figure S11** Change in interlayer distance with change in temperature

**15. Change in  $\vartheta$ ,  $\varphi$ , X and Y with change in temperature**

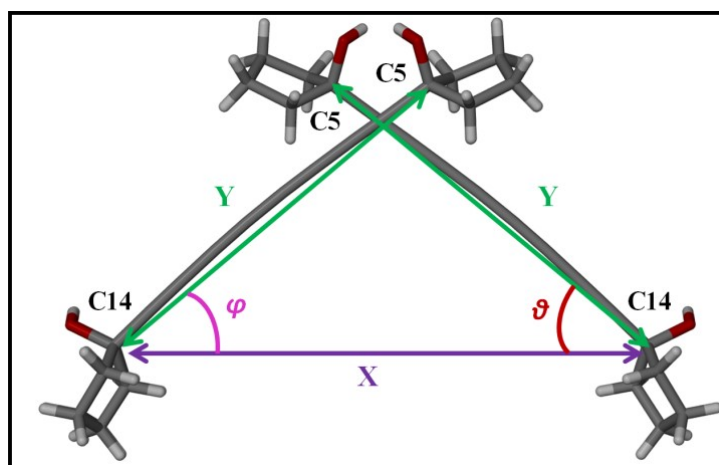


**Figure S12** Schematic representation of the mechanism showing the distance between the molecules (X) parallel to the *a*-axis, Angle of inclination ( $\vartheta$  and  $\varphi$ ) and distance between C5 to C14 *i.e.* length of the spine (Y)

**Table S6** Change in  $\vartheta$ ,  $\varphi$ , X and Y with change in temperature

Temperature (K)	Angle ( $\vartheta$ ) (°)	Angle ( $\varphi$ ) (°)	Distance (X) (Å)	Distance (Y) (Å)
100	43.10(1)	40.83(1)	15.953(3)	11.841(2)
150	42.91(1)	40.62(1)	15.968(3)	11.828(3)
200	42.77(2)	40.45(2)	15.979(3)	11.821(3)
250	42.68(2)	40.31(2)	15.979(3)	11.809(3)
300	42.65(2)	40.23(2)	15.972(4)	11.795(4)
350	42.59(2)	40.13(2)	15.962(4)	11.781(4)



**Note:** Schematic representation of angle of inclination ( $\vartheta$  and  $\varphi$ ) and distance (X and Y) are mentioned in Figure S11.

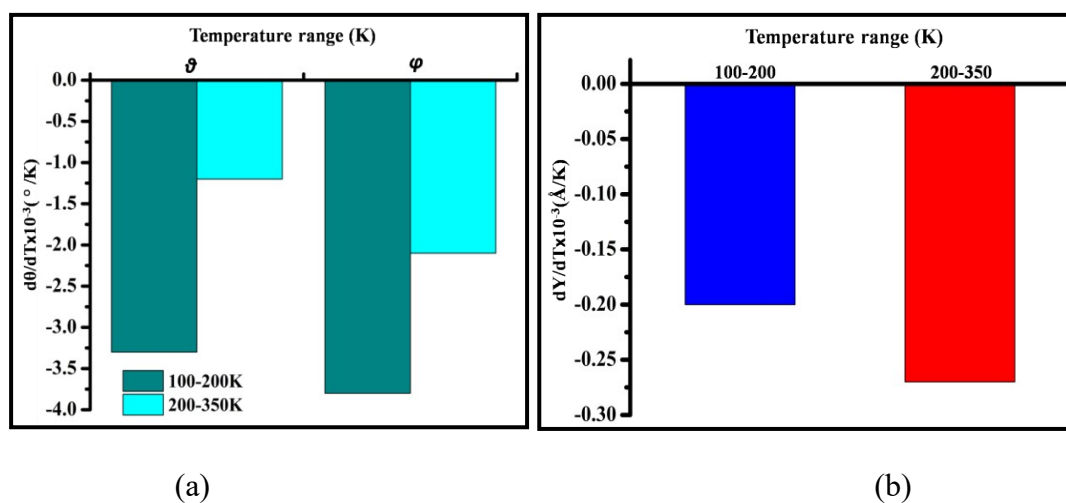


**Figure S13** Rate of change of (a) Tilt angle  $\vartheta$  and  $\varphi$  and (b) distance Y with temperature for two temperature segments

Here  $d\vartheta$  and  $d\varphi$  are the differences of the inclination angle ( $\theta$  and  $\varphi$ ) between two temperatures.  $dT$  is the difference of temperature at which data were collected.  $dY$  is the difference of the distances between C5 and C14 atoms with the change of temperature.

## 16. Calculation of Thermal Expansion Coefficients by PASCAL Program

**Table S7** Calculation of thermal expansion coefficients along different axis using PASCAL within the temperature range 100-350K

Axes	$\alpha(\text{MK}^{-1})$	$\sigma\alpha (\text{MK}^{-1})$	Direction		
			$a$	$b$	$c$
$X_1$	-5.0236	0.9552	1.0	0.0	-0.0
$X_2$	55.0733	3.2202	-0.0	-0.0	1.0

<b>X<sub>3</sub></b>	140.1264	1.8961	0.0	1.0	-0.0
<b>V</b>	194.7987	5.0938			

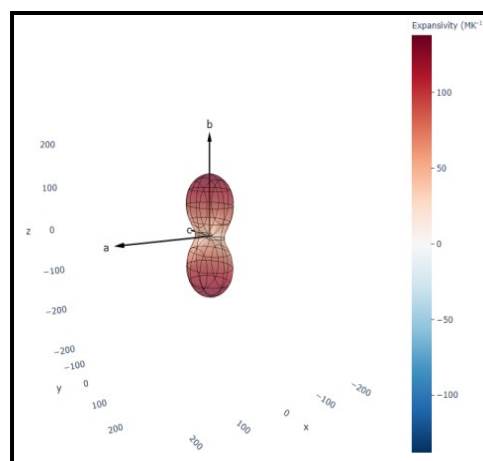
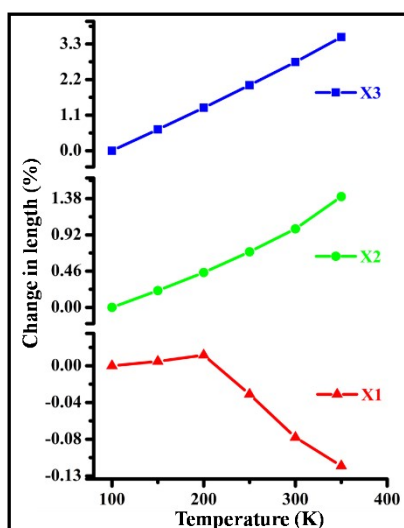
**Table S8** Calculation of thermal expansion coefficients along different axis using PASCAL within the temperature range 100-200K

Axes	$\alpha(\text{MK}^{-1})$	$\sigma\alpha (\text{MK}^{-1})$	Direction		
			<i>a</i>	<i>b</i>	<i>c</i>
<b>X<sub>1</sub></b>	1.2218	0.048	1.0	0.0	-0.0
<b>X<sub>2</sub></b>	44.2569	0.3579	-0.0	-0.0	1.0
<b>X<sub>3</sub></b>	132.9394	0.3607	0.0	1.0	0.0
<b>V</b>	180.0275	0.9641			

**Table S9** Calculation of thermal expansion coefficients along different axis using PASCAL within the temperature range 200-350K

Axes	$\alpha(\text{MK}^{-1})$	$\sigma\alpha (\text{MK}^{-1})$	Direction		
			<i>a</i>	<i>b</i>	<i>c</i>
<b>X<sub>1</sub></b>	-8.598	0.3013	1.0	-0.0	-0.0
<b>X<sub>2</sub></b>	63.6601	3.3606	-0.0	0.0	1.0
<b>X<sub>3</sub></b>	145.4669	1.6823	-0.0	1.0	-0.0
<b>V</b>	203.5899	5.8782			

**Note.** Thermal expansion coefficients were calculated using the PASCAL program.<sup>7</sup>

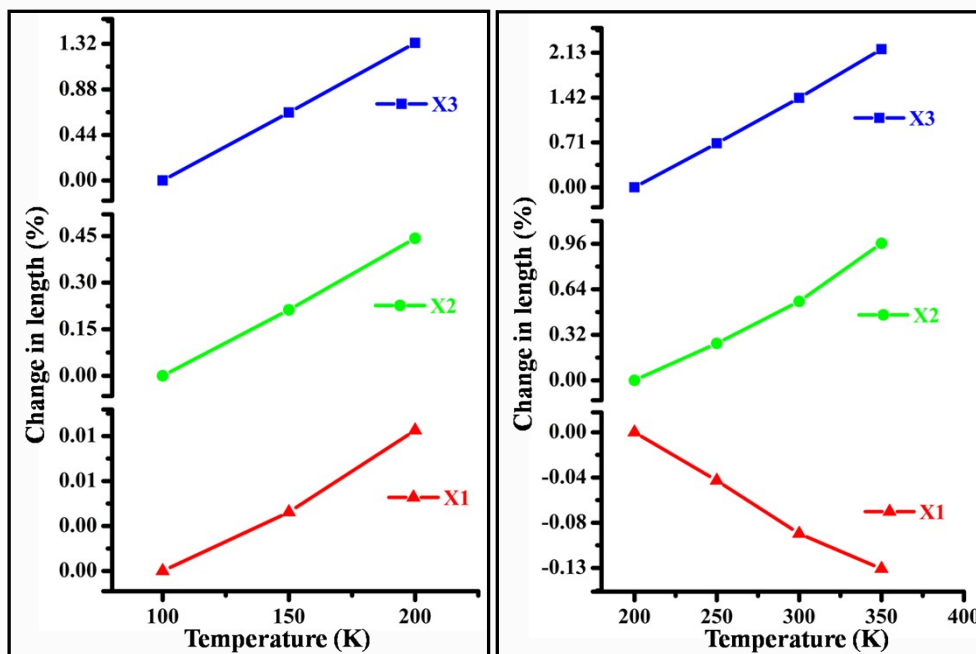


(a)

(b)

**Figure S14** (a) % change in length with change in temperature from 100-350K;

(b) Expansivity Indicatrix plot



(a)

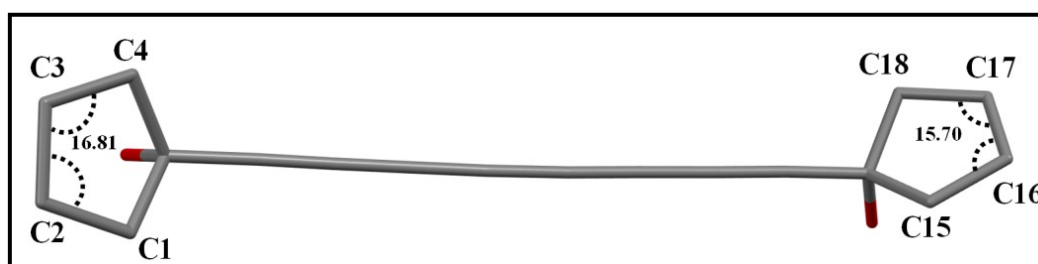
(b)

**Figure S15** (a) Percentage change in length with change in temperature from 100-

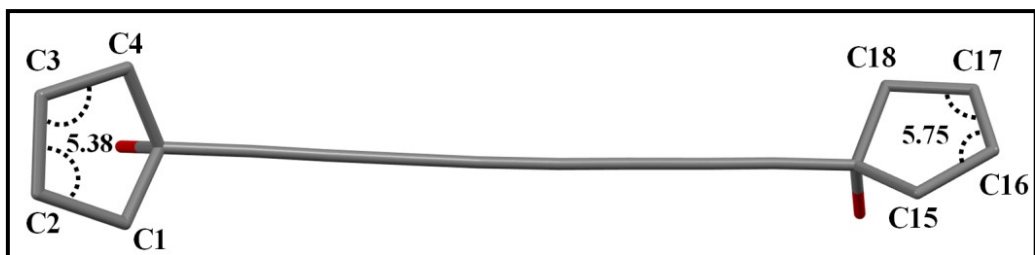
200K; (b) Percentage change in length with change in temperature from 200-350K.

## 17. Measurement of torsion angle and Cremer & Pople ring Puckering Parameters

with change in temperature from 100-350K



(a)



(b)

**Figure S16** Measurement of torsion angles C1-C2-C3-C4 and C15-C16-C17-C18 at (a) 100K and (b) 350K

**Table S10** Measurement of torsion angles C1-C2-C3-C4 and C15-C16-C17-C18 of **1** at each temperature

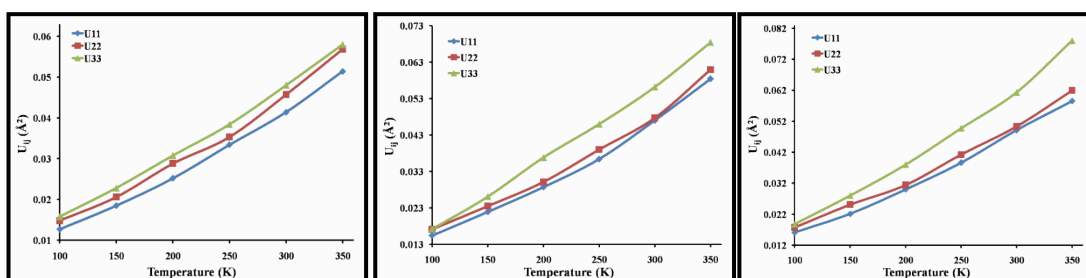
Temperature (K)	C1-C2-C3-C4 ( ° )	C15-C16-C17-C18 ( ° )
100	16.81(2)	15.70(2)
150	13.17(3)	14.16(3)
200	10.77(4)	12.43(4)
250	8.34(5)	9.68(5)
300	7.27(5)	7.60(5)
350	5.38(7)	5.75(6)

**Table S11** Measurement of Cremer & Pople ring Puckering Parameters<sup>6b</sup> from PLATON<sup>6a</sup> of **1** at each temperature

Temperature (K)	C1-C2-C3-C4-C5 Phi(2) (°)	C14-C15-C16-C17-C18 Phi(2) (°)

100	347.3(3)	337.3(3)
150	342.6(4)	338.5(5)
200	339.6(6)	340.7(6)
250	336.6(7)	344.4(8)
300	335.3(8)	347.1(9)
350	332.8(11)	349.8(12)

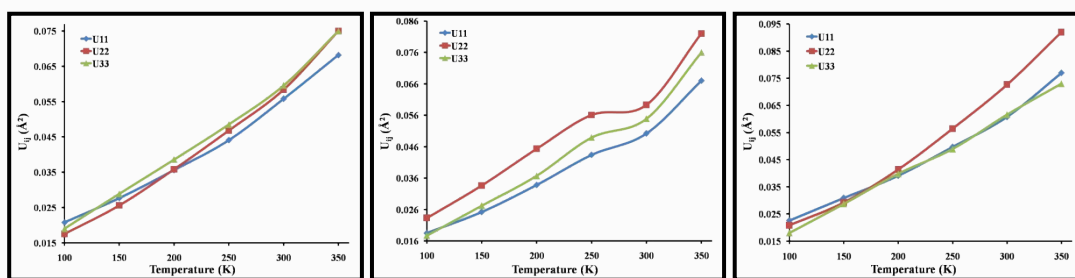
**18. Variation of anisotropic displacement parameters ( $U_{11}$ ,  $U_{22}$ ,  $U_{33}$ ) of carbon atoms with temperature**



(a)

(b)

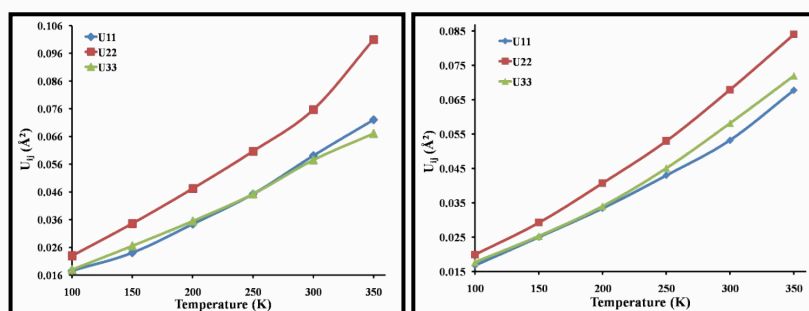
(c)

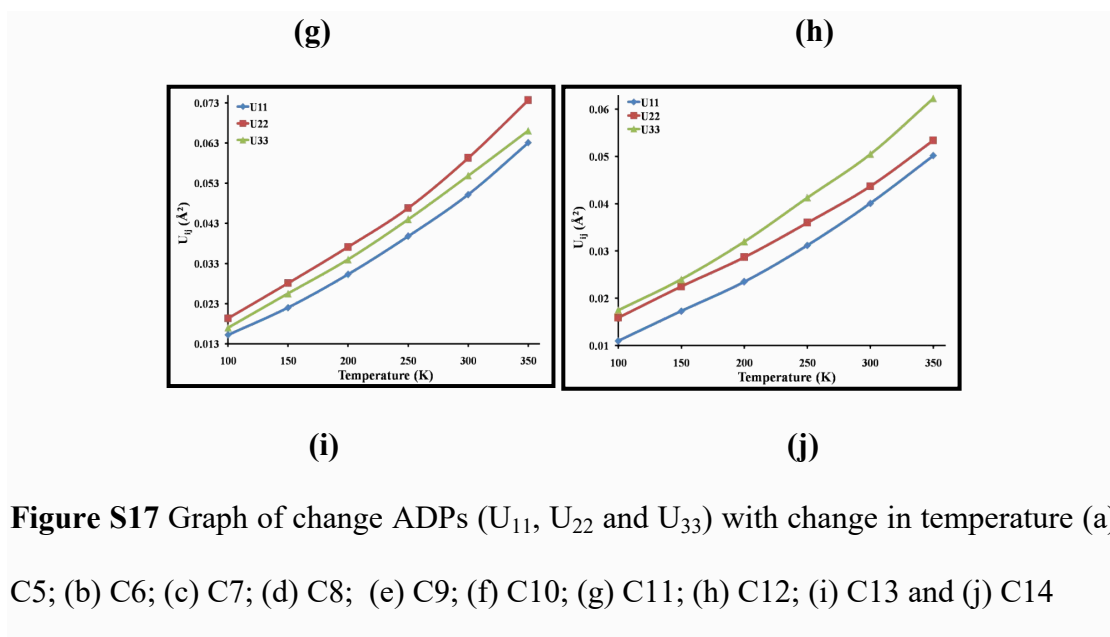


(d)

(e)

(f)





## 19. References

- (a) W. Yin; C. He; M. Chen; H. Zhang; A. Lie; *Org. Lett.*, 2009, **11**, 3; (b) S. Ghorai, D. Lee, *Org. Lett.*, 2021, **23**, 697–701.
- SAINT; Bruker AXS Inc., Madison, Wisconsin, USA, 2013. SADABS; Bruker AXS Inc., Madison, Wisconsin, USA, **2012**.
- SAINT; Bruker AXS Inc., Madison, Wisconsin, USA, 2013. SADABS; Bruker AXS Inc., Madison, Wisconsin, USA, **2012**.
- Sheldrick, G. M. SHELXTL v 2014/5; <http://shelx.uni-ac.gwdg.de/SHELX/index.php>.
- L. J. Barbour, X-Seed—A software tool for supramolecular crystallography. *J. Supramol. Chem.*, 2001, **1**, 189.
- (a) A. L. Spek, *Acta Cryst.*, 2009, **D65**, 148-155; (b) D. Cremer, J. A. Pople, *J. Am. Chem. Soc.*, 1975, **97**, 1354-1358.
- M. Lertkiattrakul, M. L. Evans, M. J. Cliffe, *J. open source softw.*, 2023, **8**, 5556.